IEEE Access
Multidisciplinary | Rapid Review | Open Access Journal

Received July 9, 2021, accepted September 8, 2021, date of publication September 16, 2021, date of current version September 29, 2021.

Digital Object Identifier 10.1109/ACCESS.2021.3113336

32 Gbps QPSK Optical Communication Technology Based on a New Equalizer in Atmospheric Turbulence

BINYU LI[1], HAIFENG YAO[2,3], LEI ZHANG[3], AND SHOUFENG TONG[3]

[1]Institute of Photoelectric Engineering, Changchun University of Science and Technology, Changchun 130022, China
[2]School of Optoelectronics, Beijing Institute of Technology, Beijing 100081, China
[3]National and Local Joint Engineering Research Center of Space Optoelectronics Technology, Changchun University of Science and Technology, Changchun 130022, China

Corresponding authors: Shoufeng Tong (cust0888@126.com) and Haifeng Yao (custfeng@outlook.com)

This work was supported by the National Natural Science Foundation of China under Grant 61775022.

ABSTRACT In this paper, cascaded least mean square-least mean square (LMS-LMS) adaptive equalization scheme is proposed based on fiber coupling system, in order to improve the transmission performance of quadrature phase shift keying (QPSK) modulated optical signals in medium and weak turbulence channels. First, the transmission performance of QPSK optical signal in different atmospheric turbulence channels is simulated and analyzed according to the characteristics of optical fiber coupling system and the characteristics of atmospheric turbulence channel. Secondly, cascaded LMS-LMS equalization scheme is proposed, and its distortion signal is corrected based on the original simulation results to verify the effectiveness and robustness of LMS-LMS. Finally, atmospheric turbulence simulator is used to verify the improvement effect of cascaded LMS-LMS adaptive equalizer under different turbulence conditions. The experimental results show that when the coherence length is $r_0 = 1.6$ cm and the received optical power is -34 dBm, the system can transfer the information at a rate of 32 Gbps QPSK after using cascaded LMS-LMS adaptive equalizer, and the bit-error ratio (BER) is lower than the minimum limit of forward error correction (FEC, 3.8×10^{-3}). This paper can provide theoretical guidance for the performance optimization of free space QPSK optical signal transmission system.

INDEX TERMS Free space optical communication, quadrature phase shift keying, atmospheric turbulence simulator, cascaded LMS-LMS adaptive equalizer.

I. INTRODUCTION

Free-space optical communication (FSOC) technology uses the laser as a carrier wave for communication, which combines the advantages of radio communication and optical fiber communication. FSOC has the advantages of strong anti-electromagnetic interference ability, high security, high communication speed, and large information capacity. It is characterized by small system size, lightweight, low power consumption, simple construction, and flexibility mobility has significant strategic needs and application value in both military and civilian fields [1]–[3]. FSOC can be used as an emergency communication solution, applied to earthquake relief, emergency, anti-terrorism, public security investigation, and other fields.

The associate editor coordinating the review of this manuscript and approving it for publication was Tianhua Xu.

Specifically, it can provide military confidential information services for multi-arms joint offense and defense, and has outstanding advantages in local warfare, battlefield networking, and information confrontation. In addition, benefiting from the advantages of high bandwidth, fast and convenient transmission, and low cost, FSOC is the best choice for solving the ''last 1 kilometer'' of information transmission and the transmission of the fifth-generation mobile communication technology (5G) small and micro base stations [3]. Because the traditional microwave satellite communication method is difficult to meet the demand of the highest transmission bandwidth of the space network of 40 Gbps - 100 Gbps, it is urgent to study the high-speed space laser network to meet the market needs [4]–[7]. In high-speed communication, multi-ary modulation technology such as multipulse pulse-position modulation/M-ary pulse amplitude modulation/M-ary phase shift keying and multilevel quadrature amplitude

modulation (MPPM/MPAM/MPSK and MQAM) can be used to increase the transmission rate [8]–[12], and orbital angular momentum (OAM) multiplexing technology can be also used to increase the frequency band utilization [13]–[19]. Radio frequency (RF) devices and technologies are mature. RF modulation information can be used at the transmitting end to modulate the optical carrier to form a radio frequency optical (RFO) network, thereby increasing the transmission rate of light, and can form multiple orthogonal carriers by RF, which can be carried out by orthogonal frequency-division multiplexing (OFDM) [20], [21]. Our research group also conducted related technical research, analyzed the transmission performance of the multi-ary modulation format in the atmospheric turbulence channel [22], [23], and adopted polarization multiplexing and quadrature phase shift keying (QPSK) multiplexing technology to achieve 384 Gbps communication. The above researches are all pursuing the multiplexing of various technologies [24], but there are atmospheric turbulence effects in self-use space channels [25], [26], which cause beam drift, random fluctuations, and spot fragmentation, which makes it difficult to use in practical engineering. When being tracked and aligned, there is a pointing error, which aggravates the influence of the received optical signal [6], [27], [28]. The least mean square (LMS) adaptive equalization technology is an effective means to correct signal distortion, but the correction ability of a single LMS is limited, and in many cases, it cannot make the communication error rate lower than forwarding error correction (FEC) 3.8×10^{-3} [19]. Therefore, we employ the cascade LMS-LMS adaptive equalizer to optimally adjust the tap coefficient to achieve the suppression of high-speed laser signal distortion. Here, we did not use any multiplexing technology only QPSK to achieve the Gbps communication in the atmospheric turbulence simulation pool.

In this paper, the LMS-LMS cascaded adaptive equalizer is used to achieve 32 Gbps information transmission in medium and weak turbulence. The Johnson S_B channel model are introduced, and the communication link based on the atmospheric turbulence simulation is established. Then the atmospheric turbulence simulator is used to verify the improvement effect of cascaded LMS-LMS adaptive equalizer under different turbulence conditions. The results can provide theoretical guidance for the performance optimization of free space QPSK optical signal transmission system.

II. SIMULATED TURBULENCE CHANNEL

In our previous work [22]–[24], [29], the Johnson S_B probability density function (PDF) was used to describe the process of spatial light coupling to a single-mode fiber as follows:

$$p(\zeta) = \frac{\delta}{\sqrt{2\pi}} \frac{1}{\zeta} \exp\left\{-\frac{1}{2}\left[\gamma + \delta \ln\left(\frac{\zeta}{1-\zeta}\right)\right]^2\right\}. \quad (1)$$

where ζ is normalized light intensity which obeys $0 < \zeta < 1$. δ and γ are free parameters which can be calculated by

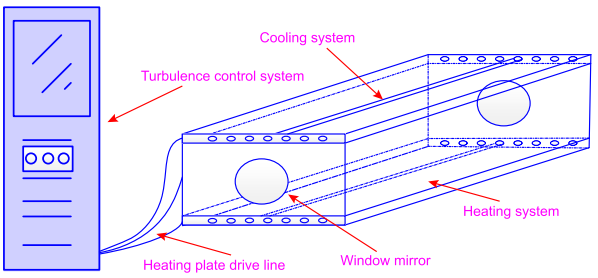

FIGURE 1. Schematic diagram of atmospheric turbulence simulation pool.

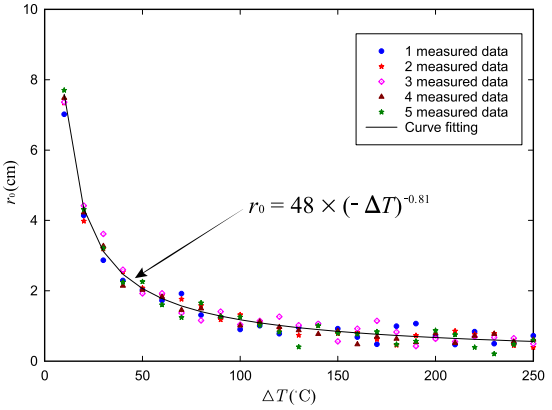

FIGURE 2. Fitting curve of atmospheric turbulence pool temperature and atmospheric coherence length, *i*-th measured data is *i*-th the numerical results of experimental measurements.

average light intensity fluctuation σ_ζ^2

$$\sigma_\zeta^2 = \left\langle \zeta^2 \right\rangle - \left\langle \zeta^1 \right\rangle^2, \quad (2)$$

$$\overline{\sigma_\zeta^2} = \frac{\left\langle \zeta^2 \right\rangle - \left\langle \zeta^1 \right\rangle^2}{\left\langle \zeta^1 \right\rangle^2}, \quad (3)$$

$$\langle \zeta \rangle = \int_0^1 \zeta^n p(\zeta) d\zeta, \quad (4)$$

where $\langle \zeta^n \rangle$ represents the n^{th} order moment of ζ, $\overline{\sigma_\zeta^2}$ is normalized fluctuation variance. Therefore, the Johnson S_B PDF is characterized the transmission performance of QPSK signal in real atmospheric optical channel. It is worth noting that we employ the atmospheric turbulence simulation pool as the source of real atmospheric turbulence, which is made up of cooling system, heating plate drive line, heating system, window mirror and turbulence. The temperature difference between the heating system and the cooling system results in turbulence disturbance in the atmosphere, which is shown as Fig. 1. 1 km turbulence link through our experimental accurate measurement and calibration can be simulated, the fitting curve of atmospheric turbulence pool temperature ΔT and atmospheric coherence length r_0 (cm), which is shown as Fig. 2, the equation is given as

$$r_0 = 48 \times (-\Delta T)^{-0.81}. \quad (5)$$

In order to explore the transmission performance of QPSK signal in real atmospheric optical channel, we depict the

schematic diagram, which is shown in Fig. 3. At the transmitter end, a tunable fiber laser (Tektronix OM2210, linewidth: 100 kHz, TL) of 1550.116 nm was used as the carrier of QPSK. Two RF signals (pseudo-random binary sequence, PRBS-15) with 16 Gbps rate were generated by an arbitrary waveform generator (AWG, Keysight M8195A), and the IQ modulator was driven to generate 32 Gbps QPSK optical signals (one was used for forward modulation, the other was used for phase difference modulation). The QPSK optical signal was amplified by erbium-doped fiber amplifier (EDFA) through optical fiber, and sent out through optical antenna as space light. At the receiver, the QPSK optical signal in atmospheric turbulence simulator was received by an optical antenna and coupled into the single mode fiber (SMF). Two band-pass filters and EDFA were used as preamplifiers (Pre-EDFA, Amonics AEDFA-23-E-FA-MAX-20dB) to amplify the optical signal in SMF, and the QPSK optical signal of appropriate power was obtained by adjusting the variable optical attenuator (VOA, EXFO FVA-3150), to complete the coherent demodulation detection. The demodulated signal was analyzed by optical modulation analyzer (Keysight N4391A), the experimental link is shown in Fig. 3.

III. DESIGN OF CASCADED LMS-LMS ADAPTIVE EQUALIZER

The noise sources mainly come from two aspects: one part is the noise from the atmospheric optical channel, it is also the main noise, the system function can be expressed as $H_{turbulence}(j\omega)$. The noise of the other part comes from the optical fiber channel and devices, which is the secondary noise [1]. Its system function can be expressed as $H_{fiber}(j\omega)$. Then the whole transmission system can be expressed as

$$\begin{aligned} Y_{qpsk}(j\omega) &= R_{qpsk}(j\omega) \cdot H_{turbulence}(j\omega) \cdot H_{fiber}(j\omega) \\ &= R_{qpsk}(j\omega) \cdot H(j\omega), \end{aligned} \tag{6}$$

The z domain of Eq. (6) can be expressed as

$$H(j\omega) = \frac{Y_{qpsk}(j\omega)}{R_{qpsk}(j\omega)} \rightarrow H(z) = \frac{Y_{qpsk}(z)}{R_{qpsk}(z)}, \tag{7}$$

Equation (7) can be rewritten through processing the digital signal

$$\begin{aligned} H(z) &= \frac{Y_{mpsk}(z)}{R_{mpsk}(z)} = \frac{\sum_{r=0}^{M} b_r z^{-r}}{1 + \sum_{k=0}^{N} a_k z^{-k}} \\ &= \frac{b_0 + b_1 z^{-1} + b_2 z^{-2} + \ldots + b_M z^{-M}}{1 + a_1 z^{-1} + a_2 z^{-2} + \ldots + a_N z^{-N}}. \end{aligned} \tag{8}$$

Since the finite sequence is convergent in z-plane ($|z| > 0$), the response $H(z)$ has no pole, all a_k in $H(z)$ must be zero, we will obtain

$$H(z) = \sum_{r=0}^{M} b_r z^{-r} = b_0 + b_1 z^{-1} + \ldots + b_M z^{-M}. \tag{9}$$

Equations (6), (7) and (9) can be written as

$$\begin{aligned} H(z) &= \sum_{r=0}^{M} b_r z^{-r} \\ &= H_{turbulence}(z) \cdot H_{fiber}(z) \\ &= \left(\sum_{n=0}^{N_1} b_{1n} z^{-n} \right) \left(\sum_{m=0}^{N_2} b_{2m} z^{-m} \right) \\ &= \left(b_{10} + b_{11} z^{-1} + \ldots b_{1N_1} z^{-N_1} \right) \\ &\quad \cdot \left(b_{20} + b_{21} z^{-1} + \ldots b_{2N_2} z^{-N_2} \right). \end{aligned} \tag{10}$$

Here, the compensation function was given

$$H_{turbulence}(z) \cdot G_{turbulence}(z) = 1, \tag{11}$$

$$H_{fiber}(z) \cdot G_{fiber}(z) = 1. \tag{12}$$

Then, we used the least mean square (LMS) adaptive equalizer to express Eqs. (11) and (12), which is given as

$$\begin{aligned} G_{turblence}(z) &= \frac{1}{H_{tubulence}(z)} = \sum_{m=0}^{M} W_{1m} z^{-m} \\ &= W_{10} + W_{11} z^{-1} + \ldots + W_{1M} z^{-M}, \end{aligned} \tag{13}$$

$$\begin{aligned} G_{fiber}(z) &= \frac{1}{H_{fiber}(z)} = \sum_{n=0}^{N} W_{2n} z^{-n} \\ &= W_{20} + W_{21} z^{-1} + \ldots + W_{2N} z^{-N}. \end{aligned} \tag{14}$$

The structure of the adaptive equalizer is shown in Fig. 4. LMS1 can compensate the distortion caused by atmospheric optical channel, and LMS2 can reduce the noise caused by fiber channel and device itself. $e_1(k)$ and $e_2(k)$ are the time domain error signals of LMS1 and LMS2. $z_1(k)$, $z_2(k)$ and $W_{1i}(k)$, $W_{2j}(k)$ are the expected signals and tap coefficients, respectively. We can get good results of Eq. (10) through cascade LMS-LMS adaptive equalizer.

IV. RESULTS AND DISCUSSION

Firstly, the performance of the system without cascaded LMS-LMS adaptive equalizer was analyzed. The received optical power was about 3 dBm, when the transmitted optical signal power was set to 12 dBm, which indicates the attenuation is 9 dB in the transmission link of the whole system. This attenuation was due to the wave front distortion of QPSK optical signal caused by atmospheric turbulence, which made the transmitted light wave and the received SMF mode mismatch, resulted in the degradation of coupling efficiency. The loss of the junction between optical devices was also an important reason. Therefore, QPSK optical signal can be amplified by pre-EDFA before coherent demodulation to meet the requirements of demodulation. In our experiment, the atmospheric coherence length of the atmospheric turbulence simulator was set to 7.8 cm, 3.2 cm and 1.6 cm, respectively. The sampling diagram of SMF receiving power jitter can be obtained and shown in Fig. 5, the sampling points is 1000 and the sampling time is 100 Hz. In Fig. 5, the average

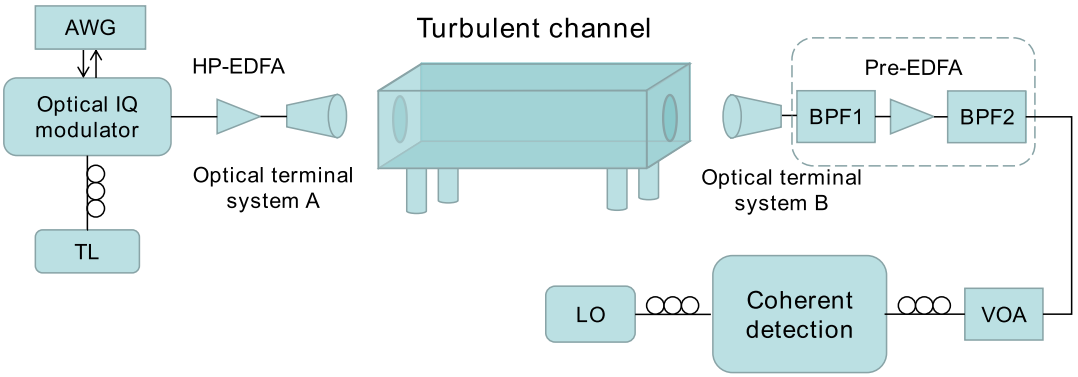

FIGURE 3. The schematic diagram of QPSK signal in real atmospheric optical channel.

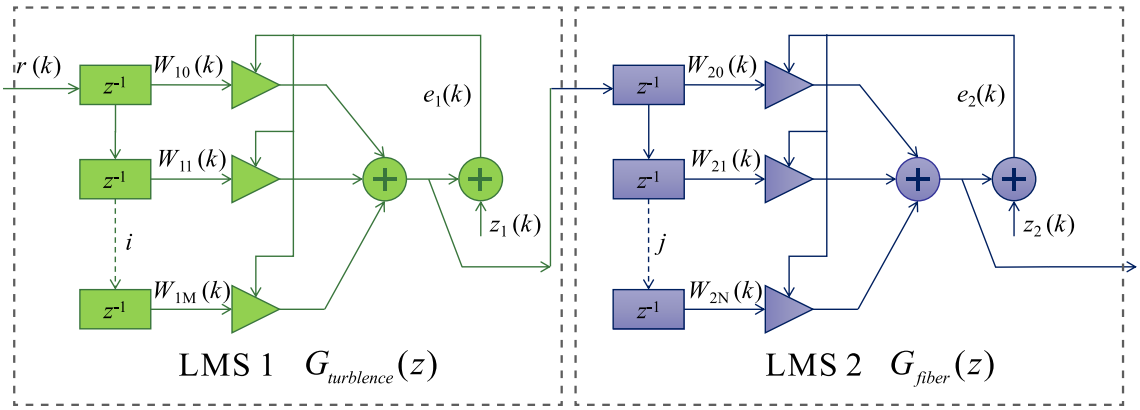

FIGURE 4. Structure diagram of cascaded LMS-LMS algorithm($i = 1, 2, \ldots M, j = 1, 2, \ldots N$), the LMS1 and LMS2 is $H_{turbulence}(j\omega)$ and $H_{fiber}(j\omega)$, respectively.

power received by SMF decreases and the power jitter amplitude increases when the atmospheric coherence length (r_0) increases. The statistical results show that the average power of Figs. 5(a)-(c) are −37.1494 dBm, −37.4288 dBm and −37.556 dBm, respectively, and the maximum normalized jitter variance are 0.0171, 0.1701 and 0.4235.

The distribution map of PDF can be obtained through normalization function analysis and shown in Fig. 6. The peak value of PDF function shifts to the left (offset to vertical axis) with the increase of turbulence intensity. The distribution of optical power range was more uneven. In Figs. 6(a)-(c), the δ and γ of Johnson S_B PDF can be calculated by Eqs. (2)-(4), which are $\delta = 4$, $\gamma = 0.5$; $\delta = 1.9$, $\gamma = 2.8$; $\delta = 1.5$, $\gamma = 4.3$, they represent the turbulence intensity are weak, medium and strong, respectively, which indicates that the optical power distribution received by the system conforms to the law when the atmospheric coherence length is 7.8 cm, 3.2 cm and 1.6 cm. The results verifies the accuracy of atmospheric turbulence simulator.

In order to analyze the data and study the communication performance of QPSK optical signal in atmospheric optical channel, the data was processed off-line and the performance of constellation diagram in different atmospheric coherent length (7.8 cm, 3.2 cm and 1.6 cm) are drawn in Figs. 7(a)-(c) show that the crosstalk degree of constellation diagram is increased significantly with the increase of turbulence intensity, resulting in the deterioration of BER are 5.5×10^{-6}, 2.9×10^{-4} and 1.2×10^{-3}, respectively. And the corresponding eye diagrams are portrayed as Fig. 8. At the same time, through observing the shape of a single constellation, we found that atmospheric turbulence not only affects the amplitude of QPSK optical signal, but also affects the phase. That means phase noise is introduced into FSOC system. This effect can be equivalent to that the phase factor of disturbance is added in complex variables.

Figure 9 is drawn for evaluating the relationship between bit error ratio (BER) and the receiving power at the same turbulence level. The BER decreases with the increase of the receiving power. The increasing of signal-to-noise ratio (SNR) indicates that the quality of QPSK optical signal communication in FSOC system can be improved by increasing the transmitting power. However, the improvement effect decrease with the increasing of turbulence degree, as shown in the curve in Fig. 9. When the atmospheric coherence length is 7.8 cm, the received optical power should greater than −36 dBm to ensure the BER of the system lower than 3.8×10^{-3}. When the atmospheric coherence length are 3.2 cm and 1.6 cm, the optical power needs about −32.5 dBm and −30 dBm, respectively. The results verifies the conclusion of the numerical simulation.

Then, the performance of LMS-LMS system was analyzed. Because of the noise in original system, a equalizer was

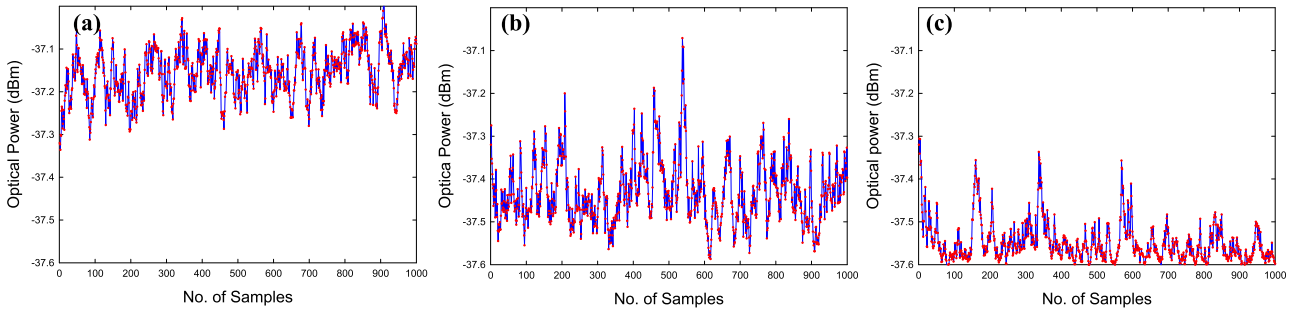

FIGURE 5. Received power sampling of QPSK optical signals in different turbulence conditions. The atmospheric coherence length of (a)-(c) are 7.8 cm, 3.2 cm and 1.6 cm, respectively.

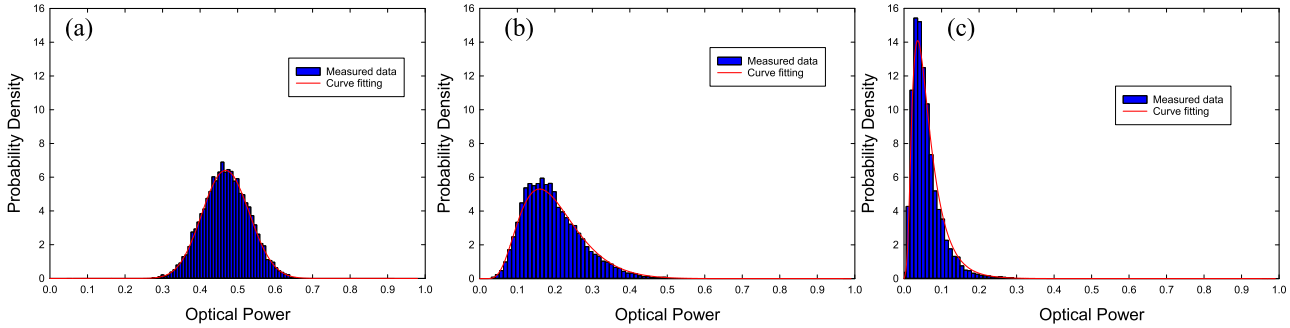

FIGURE 6. Statistical distribution of received power of QPSK optical signals under different turbulence conditions. The atmospheric coherence length of (a)-(c) are 7.8 cm, 3.2 cm and 1.6 cm, respectively.

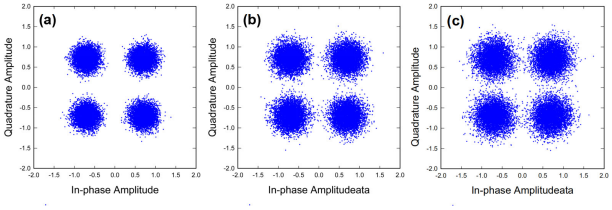

FIGURE 7. Constellation diagram of QPSK optical signals under different turbulence conditions. The atmospheric coherence length of (a)-(c) are 7.8 cm, 3.2 cm and 1.6 cm, respectively.

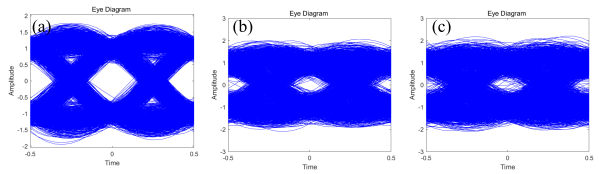

FIGURE 8. Real component eye diagram of QPSK optical signals under different turbulence conditions. The atmospheric coherence length of (a)-(c) are 7.8 cm, 3.2 cm and 1.6 cm, respectively.

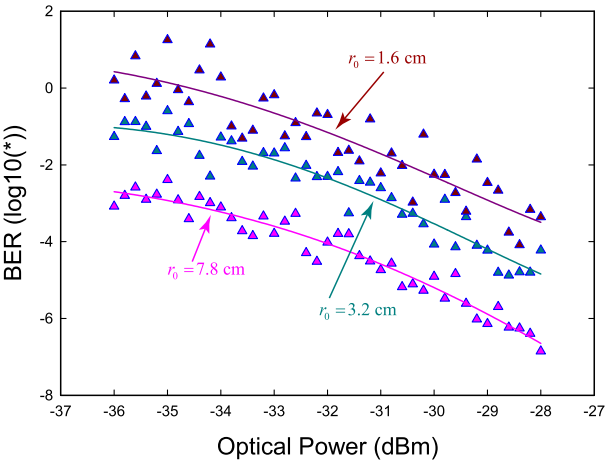

FIGURE 9. BER performance statistical diagram of QPSK optical signals under different turbulence conditions.

designed according to the principle structure shown in Fig. 4. The convergence characteristics of different step size and iteration number are shown in Fig. 10. $u = 0.01$ and $u = 0.005$ represent the step size of LMS adaptive equalizer, $u_1 = 0.005$ and $u_2 = 0.01$ represent the step size of cascade LMS-LMS adaptive equalizer.

The cascaded LMS-LMS adaptive equalizer starts to converge when the number of iterations reach about 1032. However, if a single LMS adaptive equalization is used, the number of iterations of convergence is about 10000 or 6000 when the step size is 0.01 or 0.005. It means that the convergence performance of cascaded LMS-LMS adaptive equalizer is better than single LMS. The mean square error (MSE) of cascaded LMS-LMS is about −11.5 dB, comparing with the MSE of convergence is −9.5 dB or −11 dB when the step size of single LMS is 0. 01 or 0.005. The MSE of single LMS is higher than LMS-LMS. The results show that LMS-LMS has better compensation performance. Therefore, cascaded LMS-LMS adaptive equalizer will be used to compensate the transmission of QPSK optical signal in atmospheric optical channel.

Figure 11 shows the performance of constellation diagram using cascaded LMS-LMS adaptive equalizers.

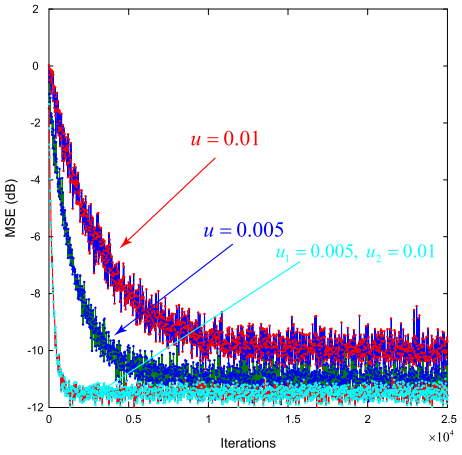

FIGURE 10. The performance of cascaded LMS-LMS adaptive equalizers with different tap coefficients and iterations.

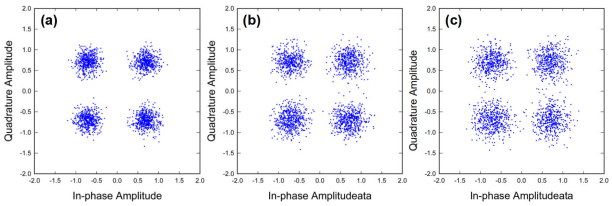

FIGURE 11. Constellation diagram of QPSK optical signals in different turbulence conditions using cascaded LMS-LMS adaptive equalizer. The atmospheric coherence length of (a)-(c) are 7.8 cm, 3.2 cm and 1.6 cm, respectively.

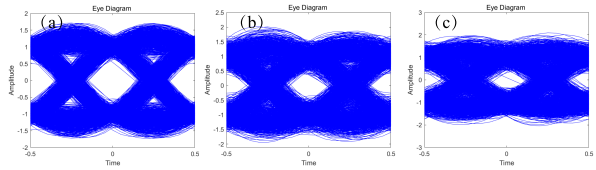

FIGURE 12. Real component eye diagram of QPSK optical signals in different turbulence conditions using cascaded LMS-LMS adaptive equalizer. The atmospheric coherence length of (a)-(c) are 7.8 cm, 3.2 cm and 1.6 cm, respectively.

The corresponding eye diagrams after the optical signal is equalized are depicted as Fig. 12. Compared with Figs. 7 and 8, it can be clearly found that the "focus" degree of constellation diagram is obviously improved after using the cascaded LMS-LMS adaptive equalizer, which indicates that the cascaded LMS-LMS adaptive equalizer can suppress the noise of QPSK optical signal transmission system and reduce BER significantly.

The BER of Figs. 11(a)-11(c) are 7.5×10^{-8}, 1.6×10^{-6} and 3.4×10^{-5}, respectively. In order to further analyze the influence of the performance of BER in the system caused by cascade LMS-LMS adaptive equalizer, the BER trend of the system after compensation are shown in Fig. 13. The improvement of BER is about -2 dB (1.1×10^{-2}) comparing with Fig. 7. When the coherence length is $r_0 = 1.6$ cm and the received optical power is -34 dBm, the BER is lower than the FEC 3.8×10^{-3} after using cascaded LMS-LMS adaptive equalizer, while the power required for compensation is -30 dBm.

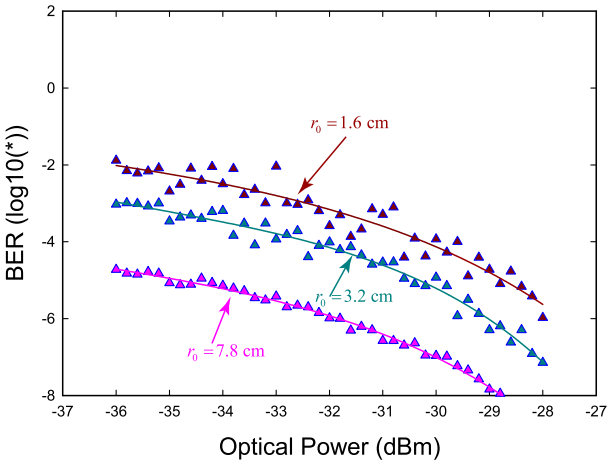

FIGURE 13. BER performance statistical diagram of QPSK optical signals in different turbulence conditions using cascaded LMS-LMS adaptive equalizer.

V. CONCLUSION

In this paper, QPSK information transmission system is proposed for atmospheric optical channel. There are two kinds of noise in the system, one is the noise caused by fiber channel and device itself, and the other is the noise caused by the turbulence effect in the atmospheric optical channel. Therefore, a cascaded LMS-LMS adaptive equalizer is proposed. The experimental results show that the cascaded LMS-LMS adaptive equalizer can suppress the system noise effectively. It is beneficial to QPSK information transmission in atmospheric optical channel. When the coherence length is 1.6 cm and the received optical power is -34 dBm, the system can transfer the information at a rate of 32 Gbps QPSK, and the BER is lower than the minimum limit of FEC (3.8×10^{-3}) after using cascaded LMS-LMS adaptive equalizer, while the power required for compensation is -30 dBm.

REFERENCES

[1] I. B. Djordjevic, *Advanced Optical and Wireless Communications Systems*. Cham, Switzerland: Springer, 2018.
[2] A. K. Rahman, A. L. Tom, N. Mohtadzar, Y. M. Buswig, N. Zamhari, D. N. A. Zaidel, S. K. Sahari, and N. Julai, "A new modulation technique to improve received power under turbulence effects for free space optical communication," *IOP Conf. Ser., Mater. Sci. Eng.*, vol. 767, Feb. 2020, Art. no. 012035.
[3] D. Anandkumar and R. G. Sangeetha, "A survey on performance enhancement in free space optical communication system through channel models and modulation techniques," *Opt. Quantum Electron.*, vol. 53, no. 1, pp. 1–39, 2021.
[4] M. Barbuto, M.-A. Miri, A. Alu, F. Bilotti, and A. Toscano, "A topological design tool for the synthesis of antenna radiation patterns," *IEEE Trans. Antennas Propag.*, vol. 68, no. 3, pp. 1851–1859, Mar. 2020.
[5] N. Zhao, X. Li, G. Li, and J. M. Kahn, "Capacity limits of spatially multiplexed free-space communication," *Nature Photon.*, vol. 9, no. 12, pp. 822–826, 2015.
[6] A. A. Algamal, H. A. Fayed, M. Mahmoud, and M. H. Aly, "Reliable FSO system performance matching multi-level customer needs in Alexandria city, egypt, climate: Sandstorm impact with pointing error," *Opt. Quantum Electrfon.*, vol. 52, no. 7, pp. 1–18, Jul. 2020.
[7] M. Jaworski, in *Proc. 16th Int. Conf. Transparent Opt. Netw.*, Graz, Austria, Jul. 2014.

[8] Y. Zhang, H. Wang, M. Cao, and Z. Bao, "Performance evaluation of MPPM-coded wireless optical MIMO system with combined effects over correlated fading channel," *Int. J. Antennas Propag.*, vol. 2020, Aug. 2020, Art. no. 7983812.

[9] H. T. T. Pham, N. T. Dang, and A. T. Pham, "Effects of atmospheric turbulence and misalignment fading on performance of serial-relaying M-ary pulse-position modulation free-space optical systems with partially coherent Gaussian beam," *IET Commun.*, vol. 8, no. 10, pp. 1762–1768, Jul. 2014.

[10] M. Abaza, R. Mesleh, A. Mansour, and H. Aggoune, "Performance analysis of MISO multi-hop FSO links over log-normal channels with fog and beam divergence attenuations," *Opt. Commun.*, vol. 334, pp. 247–252, Jan. 2015.

[11] E. E. Elsayed and B. B. Yousif, "Performance evaluation and enhancement of the modified OOK based IM/DD techniques for hybrid fiber/FSO communication over WDM-PON systems," *Opt. Quantum Electron.*, vol. 52, no. 9, Sep. 2020, Art. no. 7983812.

[12] in *Proc. 4th Int. Conf. Electr. Energy Syst. (ICEES)*, Chennai, India, Feb. 2018. [Online]. Available: http://ieeexplore.ieee.org/servlet/opacpunumber=8419658

[13] J. Xu, "Degrees of freedom of OAM-based communication systems," in *Proc. IEEE Int. Symp. Antennas Propag. USNC/URSI Nat. Radio Sci. Meeting*, Jul. 2017, pp. 1157–1158.

[14] D. K. Nguyen, O. Pascal, J. Sokoloff, A. Chabory, B. Palacin, and N. Capet, "Antenna gain and link budget for waves carrying orbital angular momentum," *Radio Sci.*, vol. 50, pp. 1165–1175, Nov. 2015.

[15] M. Oldoni *et al.*, "Space-division demultiplexing in orbital-angular-momentum-based MIMO radio systems," *IEEE Trans. Antennas Propag.*, vol. 63, no. 10, pp. 4582–4587, Oct. 2015.

[16] D. A. B. Miller, "Better choices than optical angular momentum multiplexing for communications," *Proc. Nat. Acad. Sci. USA*, vol. 114, no. 46, pp. E9755–E9756, Nov. 2017.

[17] K. Liu, Y. Cheng, X. Li, and Y. Jiang, "Passive OAM-based radar imaging with single-in-multiple-out mode," *IEEE Microw. Wireless Compon. Lett.*, vol. 28, no. 9, pp. 840–842, Sep. 2018.

[18] H. Huang, G. Milione, M. P. J. Lavery, G. Xie, Y. Ren, Y. Cao, N. Ahmed, T. an Nguyen, D. A. Nolan, M.-J. Li, M. Tur, R. R. Alfano, and A. E. Willner, "Mode division multiplexing using an orbital angular momentum mode sorter and MIMO-DSP over a graded-index few-mode optical fibre," *Sci. Rep.*, vol. 5, Oct. 2015, Art. no. 14931.

[19] M. P. Lavery, F. C. Speirits, S. M. Barnett, and M. J. Padgett, "Detection of a spinning object using light's orbital angular momentum," *Science*, vol. 341, no. 6145, pp. 537–540, 2013.

[20] M. Singh and J. Malhotra, "Long-reach high-capacity hybrid MDM-OFDM-FSO transmission link under the effect of atmospheric turbulence," *Wireless Pers. Commun.*, vol. 107, no. 4, pp. 1549–1571, Aug. 2019.

[21] H. Lei, Z. Dai, K.-H. Park, W. Lei, G. Pan, and M.-S. Alouini, "Secrecy outage analysis of mixed RF-FSO downlink SWIPT systems," *IEEE Trans. Commun.*, vol. 66, no. 12, pp. 6384–6395, Dec. 2018.

[22] H. Yao, X. Ni, C. Chen, B. Li, X. Feng, X. Liu, Z. Liu, S. Tong, and H. Jiang, "Performance analysis of MPSK FSO communication based on the balanced detector in a fiber-coupling system," *IEEE Access*, vol. 7, pp. 84197–84208, 2019.

[23] H. Yao, X. Ni, C. Chen, B. Li, X. Zhang, Y. Liu, S. Tong, Z. Liu, and H. Jiang, "Performance of M-PAM FSO communication systems in atmospheric turbulence based on APD detector," *Opt. Exp.*, vol. 26, no. 18, pp. 23819–23830, 2018.

[24] X. Liu, T. Wang, P. Lin, J. Chen, X. Zhang, H. Yao, Q. Fu, J. Yang, and H. Jiang, "Up to 384 Gbit/s based on dense wavelength division multiplexing of 100-GHz channel spacing free space laser transmission performance in a simulated atmosphere channel with adjusted turbulence," *Opt. Eng.*, vol. 57, no. 10, p. 1, Oct. 2018.

[25] P. Vaveliuk, B. Ruiz, and A. Lencina, "Limits of the paraxial approximation in laser beams," *Opt. Lett.*, vol. 32, no. 8, pp. 927–929, 2007.

[26] M. Singh, M. L. Singh, G. Singh, H. Kaur, Priyanka, and S. Kaur, "Modeling and performance evaluation of underwater wireless optical communication system in the presence of different sized air bubbles," *Opt. Quantum Electron.*, vol. 52, no. 12, pp. 1–15, Dec. 2020.

[27] E. E. Elsayed and B. B. Yousif, "Performance enhancement of the average spectral efficiency using an aperture averaging and spatial-coherence diversity based on the modified-PPM modulation for MISO FSO links," *Opt. Commun.*, vol. 463, May 2020, Art. no. 125463.

[28] A. A. Farid and S. Hranilovic, "Outage capacity optimization for free-space optical links with pointing errors," *J. Lightw. Technol.*, vol. 25, no. 7, pp. 1702–1710, Jul. 1, 2007.

[29] H. Yao, C. Chen, X. Ni, S. Tong, and H. Jiang, "Analysis and evaluation of the performance between reciprocity and time delay in the atmospheric turbulence channel," *Opt. Exp.*, vol. 27, no. 18, pp. 25000–25011, Sep. 2019.

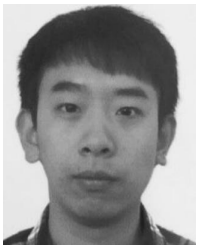

BINYU LI received the B.S. degree from the School of Science, Changchun University of Science and Technology, Changchun, China, in 2015, where he is currently pursuing the Ph.D. degree. His research interests include free-space communications, design of communication circuit, modeling and simulation of light propagation in complex environments, and the field of coherent detection.

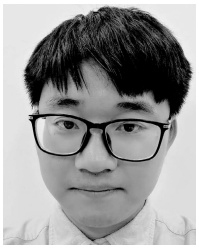

HAIFENG YAO received the Ph.D. degree from the Department of Electronic Information, Changchun University of Science and Technology, Changchun, China. He currently holds a postdoctoral position with the School of Optoelectronics, Beijing Institute of Technology. His research interests include free-space optical communications, design of communication circuit, modeling and simulation of light propagation in complex environments, and the field of coherent detection.

LEI ZHANG received the Ph.D. degree from the Department of Electronic Information, Changchun University of Science and Technology, Changchun, China. He is currently a Professor with Changchun University of Science and Technology. His current research interest includes the areas of free-space communications.

SHOUFENG TONG received the Ph.D. degree from the Department of Electronic Information, Changchun Institute of Optics, Fine Mechanics and Physics, Chinese Academy of Sciences, Jilin, China. He is currently a Professor with Changchun University of Science and Technology. He currently specializes in optical engineering, and is the provincial key leader of a team responsible for teaching in that field. His current research interests include laser communication and telemetry remote sensing technology. He was a recipient of the Yangtze River Scholar Award and successfully won the 2014 National Talent Project, in 2014.